Journal of
Engineering Sciences
Faculty of Engineering
Assiut University
JES
مجلة
العلوم الهندسية
كلية الهندسة
جامعة أسيوط
journal homepage: http://jesaun.journals.ekb.eg

# Evaluating the Accuracy of Change detection Using Spectral Indices and spectral classification, A Case Study of Fayoum Governorate, Egypt

Received 03 May 2024; Revised 18 June 2024; Accepted 18 June 2024

**Ahmed A. Elashiry** [1]

**Keywords**
Satellite images, Land cover, Spectral indices, Changes detection, Supervised classification.

**Abstract:** Spectral indices developed to extract features from satellite images are simple and fast methods that reduce processing time compared to traditional satellite image classification. In this paper, the effectiveness of the normalized difference building index (NDBI), the normalized difference vegetation index (NDVI), and the Normalized Difference Water Index (NDWI) were evaluated in land cover mapping and detecting its changes in the period from 2013 to 2023 in Fayoum Governorate, Egypt, using Landsat 8-OLI images. The results of supervised classification showed a decrease in green areas between 2013 and 2023 by 76.03 square kilometers, with a slight decrease in the areas occupied by water amounting to 3.8 square kilometers and an increase in built-up areas by 79.83 square kilometers, at the expense of green lands. On the other hand, the results of using spectral indices showed a decrease in green areas between 2013 and 2023 by 91.12 square kilometers, with a slight decrease in the areas occupied by water amounting to 3.35 square kilometers. Meanwhile, it was noticed that, increasing in the built-up areas by 94.47 square kilometers at the expense of green areas. The results showed a general convergence in the changes in the studied classes during the study period, with a great convergence in the change in the area of the water bodies resulted from the classification and from the NDWI and a convergence in the effectiveness of both the NDVI and NDBI. Finally, the effectiveness of the spectral indices in land cover mapping using check points was evaluated. The results showed a high percentage of the number of correctly identified check points for the NDWI index, with this percentage being noticeably low in the case of the NDVI and NDBI.

## 1. Introduction

The study of Land Cover (LC) change is considered an important method used by various approaches to manage and develop different natural resources. These changes are driven by

[1] Faculty of Engineering, Beni-Suef University, Beni-Suef, Egypt. eng.ahmedashiry@gmail.com

https://doi.org/ 10.21608/jesaun.2024.286600.1333

population growth and various natural, social, economic, and political factors, resulting in the expansion of urban areas at the expense of agricultural land, forests, and pastures [1]. Therefore, various methods such as traditional surveying, aerial photogrammetry, and remote sensing are employed to derive maps of land cover patterns. These methods utilize available data from remote sensing imagery to gather information about the Earth's surface from a distance. [2]. The use of satellite imagery in producing land cover maps has wide-ranging advantages, utilizing different parts of the electromagnetic spectrum to represent land cover phenomena in the form of maps. This approach offers low-cost options, particularly for large-scale areas [3]. On the other hand, GIS software provides the ability to express these phenomena in the form of databases with analysis tools that aid in understanding the relationships between land cover phenomena and their uses. It also helps clarify the direction, location, extent, and nature of changes in land cover [3 and 4].

The common approach used to derive land cover maps and detect its changes using remote sensing imagery is through a process called classification. This involves categorizing the captured imagery at different time intervals into distinct land cover classes. The process of land cover classification utilizes various algorithms, including supervised classification and unsupervised classification [6]. Each of these algorithms has its own statistical and mathematical models. In addition, classification results vary depending on the algorithms used. Unsupervised algorithms do not require any prior knowledge about the study area and rely only on the specifications of reflection. On the other hand, supervised classification requires the use of training samples, which are representative of each phenomenon of the Earth's surface, and they are collected based on the user's familiarity with the captured scene [7]. There are many algorithms used in supervised classification, and the Maximum Likelihood algorithm is considered the effective and most accurate method for land cover classification. It relies on maximum likelihood probability to determine the class to which each pixel in the image belongs based on spectral values [8].

In any case, image classification (supervised and unsupervised classification) is a lengthy and complex process that requires spectral bands composition and the application of various operations to obtain the final result. On the other hand, another approach using remote sensing imagery in studying land cover and its changes involves the utilization of spectral indices. These include the Normalized Difference Vegetation Index (NDVI) for assessing vegetation variations [9], the Normalized Difference Building Index (NDBI) for gauging urban area growth [10], the Normalized Difference Water Index (NDWI) for detecting water bodies [11], the Bare Soil Index (BSI) for identifying bare soil areas [12], and other similar indices. The use of spectral indices in studying land cover is considered easier than visual classification as it involves simple formulas that are expressed as ratios between spectral bands. This research aims to compare the results of applying these indices to derive land cover maps and sense their changes in Fayoum Governorate in the Arab Republic of Egypt. The accuracy of these maps was evaluated by comparing them with the results of supervised classification using the Maximum Likelihood method.

### 2- Research objectives and its importance

The objective of this study is to evaluate the effectiveness of using spectral indices in deriving land cover maps and sensing changes in it. This objective can be further elaborated into the following sub-objectives:

- Identifying the main land cover types in the study area using spectral indices (NDVI, NDBI, and NDWI) based on Landsat 8 OLI imagery covering the study area and acquired at different time periods, namely 2013 and 2023.
- Detecting changes in land cover in the study area during the time period from 2013 to 2023.
- Assessing the effectiveness of spectral indices in deriving land cover maps and detecting changes by comparing them with the results of the maximum likelihood supervised classification method.

The significance of the research lies in the discussion of the effectiveness of a simple method in deriving land cover maps and detecting changes, which serves as an important input in various applications such as planning, resource management, and studying urban expansion.

## 2. Previous Studies

Spectral indices have been used in numerous studies for classifying individual or multiple land cover categories from satellite imagery. Szabo et al., 2016, verified three spectral indices, namely NDVI, NDWI, and MNDWI (Modification of Normalized Difference Water Index), based on the following land cover types: Water bodies, cultivated lands, forests, vineyards, meadows, and built-up areas were classified using Landsat-7 ETM+ satellite data. The study concluded that it is possible to distinguish different land cover phenomena, albeit with some overlap, especially when dealing with vegetation types with varied water content. The study also indicated that the MNDWI index is more effective in highlighting water bodies [13]. Abdel-Gawad et al., 2019, analyzed the changes that occurred in land cover patterns and land use, especially agricultural lands, from 1989 to 2014 using the NDVI and NDBI indices. The study resulted in a digital geographic database for land cover phenomena and a digital map for environmentally degraded agricultural lands [14]. Al-Khaqani et al., tested some techniques for detecting changes, including NDVI, NDBI, and NDWI, to classify three main categories of land cover: vegetation, water bodies, and built-up areas, using Landsat ETM satellite data. The results were compared to those of an unmonitored classification. The study concluded that the investigated phenomena were well isolated [15]. Yasin et al., 2022 used Landsat data to evaluate urban growth temporally and spatially using the spectral indices NDVI and NDBI [16]. The research proved that using these two indicators improves the accuracy of analyzing land cover changes. Shoukat et al., 2022 studied the relationship between the NDVI and NDBI indices by analyzing a set of Landsat 8 OLI/TIRS imagery at different times. The results of the study revealed a negative correlation between these two indices. Additionally, the study showed that the NDBI index is highly effective in detecting urban areas [17]. Sinha et al., 2016 proposed a technique to extract the urban area built-up from Landsat Thematic Mapper (TM) and Enhanced Thematic Mapper Plus (ETM+) time

series images, and to identify changes in urban areas from 1984 to 2015. The study selected three indices: the Enhanced Built-Up and Bareland Index (EBBI), the Soil-Adjusted Vegetation Index (SAVI), and the Modified Normalized Difference Water Index (MNDWI), to represent four major phenomena in land cover: built-up areas, bare land, open water bodies, and vegetation cover. The results indicated the effectiveness of the EBBI index in accurately and easily extracting built-up areas [18]. Finally, Li et al., 2017, proposed a spectral index for automatic extraction of bare land from Landsat satellite imagery without the need for training samples. This index overcomes the problems caused by traditional indices used in this process. The underlying problem that this research attempted to solve is the difficulty in visually distinguishing between bare earth and built-up areas in one image due to their high complexity and similarity in spectral response patterns [19].

Our study differs from the previous studies as it aims to clarify the effectiveness of a set of spectral indices in deriving land cover classes and detecting changes. This is achieved by comparing the results of applying these indices with reference visual interpretations and the classification results of Landsat 8 OLI imagery, where it is not just studying the relationship between these indices or comparing their application results with the results of an unsupervised classification. This will enable us to evaluate more accurately and comprehensively the effectiveness of these indices in classifying land cover in the study area and sensing its changes within the used period in the research.

## 4. Study methods and materials

### 4.1 The study area

The spatial framework of this research is part of the Faiyum Governorate in the Arab Republic of Egypt, which extended between longitude lines 30º 20′ and 31º 10′ East, and latitude lines 29º 20′ and 29º 35′ North (Figure 1). It is located about 90 km southwest of Cairo, bordered by Giza to the north and east, and Beni Suef to the south. The Western Desert represents its western boundary [20]. The approximate area of the study area is 2002.58 square kilometers. The area is characterized by an urban fabric consisting of urban areas, green areas, and barren land, with some large water bodies present.

### 4.2 NDVI, NDBI and NDWI Spectral indices

Spectral ratios or indices are mathematical structures used to quickly extract information about the dynamics of the Earth's surface in multispectral satellite imagery, using multiple spectral bands of the electromagnetic spectrum. The main objective of using these indicators is to enhance the spectral characteristics of features in the visual imagery, regardless of the contrast in scene illumination. They are used to extract phenomena from satellite imagery to track changes in their pattern [21]. Spectral indices are mathematical combinations of reflectance values at different wavelengths that enhance the contrast between different land cover types and surface conditions. They are vital tools in scientific research and have diverse applications that significantly benefit society by enhancing detection of agricultural

productivity, recognition of natural resources, aiding in disaster response, and supporting sustainable development.

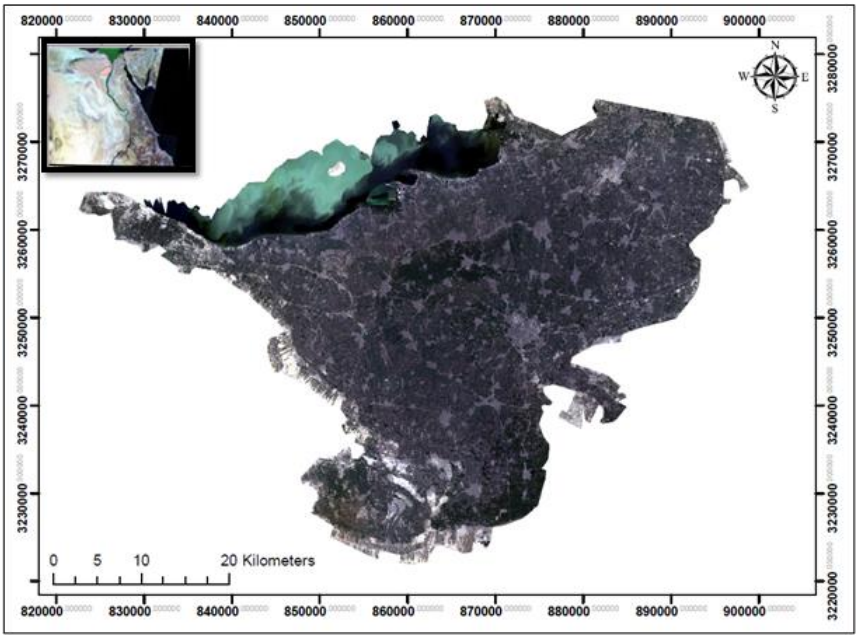


Figure 1. The study area

Many researchers have utilized the NDVI index to map and monitor green areas using satellite imagery [22, 23, 24 and 25]. The values of this index range between -1 and +1, depending on the Digital Number (DN) values of the Near Infrared and Red bands [22]. The negative values of this index, which fall within the range of 0.1-0.2, correspond to rocks, clouds, snow, water surfaces, and bare land. Healthy and dense plants have a positive value of approximately 0.5, while scattered plants have positive values ranging from 0.2 to 0.5. On the other hand, moderately dense plants have positive values ranging from 0.4 to 0.6. Values greater than 0.6 indicate the highest possible density of plants [26]. The NDVI (Normalized Difference Vegetation Index) is calculated using the following relationship:

$$NDVI = \frac{NIR-RED}{NIR+RED} \quad (1)$$

Where NIR is (band 5) and RED is (band 4)

The NDBI index is used for extracting, mapping, and monitoring built-up areas based on satellite images. Built-up areas have higher spectral reflectance within the medium infrared (MIR) range, which ranges from approximately 1.55 to 1.75 μm. The values of this index range between -1 and +1 [27]. Positive values of this index are consistent with built-up areas, and the higher the value, the stronger the indication of these areas. This index can be calculated using the following equation:

$$NDBI = \frac{SWIR-NIR}{SWIR+NIR} \quad (2)$$

Where SWIR is (band 6)

As for the NDWI index, it is used to distinguish water areas from other land surface features. The spectral reflectance of water is high in the green wavelength range, which ranges from 0.52 µm to 0.6 µm, and low in the near-infrared wavelength range, which ranges from 0.76 to 0.9 µm. The values of this index range between -1 and +1 [28], and positive values of this index correspond to water areas. The positive values of this index correspond to water bodies, and the larger the value, the stronger the indication of these areas. This index can be calculated using the following equation:

$$NDWI = \frac{Green - NIR}{Green + NIR} \qquad (3)$$

Where GREEN is (band 3)

### 4.3 Research Methodology

The approach followed in this research is the experimental method, which investigates the causal relationships between variables that may have an impact on the formation of the phenomenon or event. The experimental method aims to determine the combined effect of the factors under study on the phenomenon. Regarding the research variables, they are the spectral indices NDVI, NDBI, and NDWI, which were studied in this research to assess their effectiveness in mapping land cover phenomena in order to study their changes during the study period. The steps of the research methodology are summarized in figure 2.

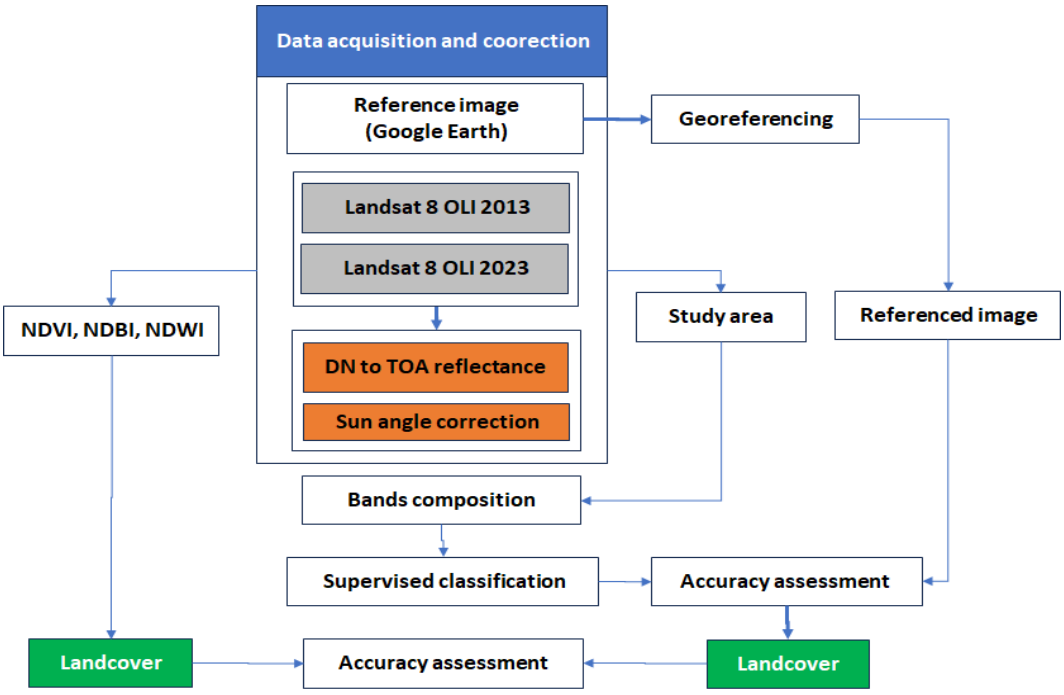


Figure2. Research Methodology

Regarding data collection, two Landsat 8-OLI images were used, captured in the years 2013 and 2023 respectively, for the study area. Where the images used in the analyses were taken on 15/4/2013 and 15/4/2023, respectively.

Each image consists of eleven spectral bands with a spatial resolution of 30 m, except for the Panchromatic band (band 8) with a spatial resolution of 15 m (Table1). These two images were downloaded from the Earth Explorer website (https://earthexplorer.usgs.gov), which belongs to the United States Geological Survey (USGS).

Table (1). The most important spectral bands for Landsat 8.

| Bands | Wavelength, (µm) | Resolution, (m) |
|---|---|---|
| Band 1 – Coastal aerosol | 0.45-0.43 | 30 |
| Band 2 - Blue | 0.51-0.45 | 30 |
| Band 3 - Green | 0.59-0.53 | 30 |
| Band 4 - Red | 0.67-0.64 | 30 |
| Band 5 – Near Infrared (NIR) | 0.88-0.85 | 30 |
| Band 6 -SWIR 1 | 1.65-1.57 | 30 |
| Band 7 -SWIR 2 | 2.29-2.11 | 30 |
| Band 8 - Panchromatic | 0.68-0.50 | 15 |
| Band 9 - Cirrus | 1.38-1.36 | 30 |

Then, the digital number (DN) values of each band of the Landsat 8 imagery were converted to reflectance values and corrected for the effects of sun elevation angle. In fact, during the transmission of electromagnetic radiation through the atmosphere to satellite sensor devices, gases and atmospheric aerosols cause absorption and scattering of this radiation [29]. Therefore, correcting the sun elevation angle and atmospheric effects on the satellite imagery is an important step in the preprocessing of these images before proceeding with the analysis [30]. The process of TOA (Top of Atmosphere) corrections or converting from digital numbers (DN) to reflectance values, reduces the effects of the atmosphere on the imagery and provides TOA reflectance products. These corrections interpret the differences resulting from acquisition time, weather conditions, and the positions of the sun, Earth, and the satellite. The equation for converting from DN to reflectance with correction for sun elevation angle is given as follows:

$$TOA_{reflectance} = (M_\rho . DN + A_\rho)/Sin(\gamma) \qquad (4)$$

Where: $M_\rho$ is the reflection of the band, DN is the values of the digital numbers stored in the specific band, $A_\rho$: is the additional reflection specific to the band, and $\gamma$ is the Sun Elevation angle.

The previous values can be obtained from the accompanying metadata, specifically the metadata associated with Landsat 8 visual data. Additionally, two images had been extracted from the free web browser Google Earth that cover the study area during the study period with a resolution of 10 meters to serve as reference images necessary for evaluating the accuracy of the visual classification used in this research. The image registration process has been performed to transfer these images to the same coordinate system of Landsat 8 OLI for the years 2013 and 2023, respectively. This process was accomplished by registering the images using 12 common control points between Landsat 8 OLI and Google Earth images

and applying a second-order polynomial transformation using the ArcGIS 10.8 software. (Table 2) illustrates the results of the image registration process.

Table (2). Results of Satellite image registration

| Visual | Number of control points. | Polynomial Transformation Degree | Horizontal Mean Squared Error $RMS_T$ |
|---|---|---|---|
| **Google Earth image 2013** | 12 | Second | 35.06 m |
| **Google Earth image 2023** | 12 | Second | 32.59 m |

To assess the accuracy of geometric correction, a tolerance threshold is given for the geometric retrieval of satellite images according to the relationship [31]:

$$RMS_T \leq (4 \rightarrow 6).GR(in\ meters) \quad (5)$$

Where GR is the Ground Resolution of the image. Applying the relationship, it was found that; the tolerance limits for Google Earth images range from 40 m to 60 m, and therefore the retrieval results are acceptable. Threshold values for indices used in land cover classification can vary depending on the specific study area and the objectives of the analysis. However, common threshold values used in many studies are:

*NDVI (Normalized Difference Vegetation Index)*
- Threshold for vegetation: (NDVI $>$ 0.2)
- Values above 0.2 typically indicate the presence of vegetation.
- Higher values (e.g., above 0.5) indicate dense vegetation.

*NDBI (Normalized Difference Built-up Index)*
- Threshold for built-up areas :( NDBI $>$ 0)
- Positive values often indicate built-up or urban areas.
- Higher positive values (e.g., above 0.1) can be used to delineate more clearly defined built-up regions.

*NDWI (Normalized Difference Water Index)*
- Threshold for water bodies: (NDWI $>$ 0)
- Positive values usually indicate the presence of water.
- Higher positive values (e.g., above 0.3) are often used to confirm the presence of water bodies.

Next, the Bands composite bands for Landsat 8 OLI were installed for the years 2013 and 2023, and the study area was extracted. Then, the training samples were extracted for the approved varieties in the study, and the supervised classification was implemented for both visual images to obtain land cover maps for the years 2013 and 2023 respectively, using the

same number of training samples. This was done after evaluating the accuracy of these samples. In addition, the spectral indices NDVI, NDBI, and NDWI were used to derive maps of green areas, buildings, and water respectively, based on the Landsat 8 OLI imagery for the years 2013 and 2023, respectively. Finally, comparisons have been made between the results of the monitoring classification and the results of applying spectral indices to determine their effectiveness in sensing changes in land cover.

## 5. Results and discussion

Training samples were measured to represent the different land cover classes. These samples were selected across various locations to ensure an adequate and appropriate number for the classification process. As for the categories that have been adopted in this study, they are indicated in Table (3).

Table (3). Land cover classes used in the research.

| Land cover type | Description |
|---|---|
| Built-up (urban areas) | Residential areas and road network. |
| Vegetation | Farmlands and Trees |
| Water | Water areas / rivers |

### 5.1 Landsat 8 imagery classification for the year 2013.

The classification of Landsat 8 satellite imagery captured for the study area in the year 2013 was performed using the maximum likelihood algorithm and the spectral signature file of the samples that were measured in the imagery. The same number of samples, 20 samples, were measured for each class category. The Contingency matrix was calculated to evaluate the quality of the samples used. It was found that; from (Figure 3) all the categories that have been assigned are located within more than 95% within different groups and that there is no overlap between the categories. Therefore, the chosen samples are considered acceptable.

ERROR MATRIX

| | Reference Data | | | |
|---|---|---|---|---|
| Classified Data | Buillt_Up | Vegetation | Water | Row Total |
| Buillt_Up | 98.74 | 3.82 | 3.06 | 570 |
| Vegetation | 1.26 | 96.18 | 0.00 | 410 |
| Water | 0.00 | 0.00 | 96.94 | 190 |
| Column Total | 555 | 419 | 196 | 1170 |

Figure 3. Evaluation report on the accuracy of Landsat 8 visual training samples for the year 2013.

After verifying the accuracy of the training samples, the Landsat 8 imagery were classified using the maximum likelihood method. The results of this classification are illustrated in (Figure 4). The classification accuracy was evaluated using the reference image that covers the study area. The confusion matrix or error matrix was generated using 100 check points measured on the classified imagery. Then, the file was opened, and these classified points were compared to the true reference points from the reference imagery. The overall accuracy for the classification reached 88.3%, while the kappa coefficient value was 0.90.

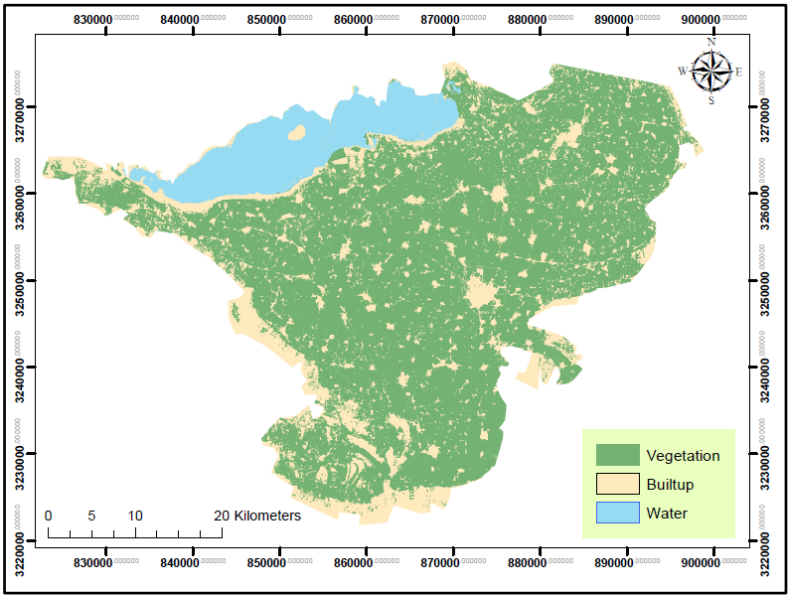


Figure 4. Results of Landsat 8 OLI maximum likelihood classification for the year 2013.

## 5.2 Landsat 8 imagery classification for the year 2023

As in the previous case, the classification of Landsat 8 satellite imagery captured for the study area in the year 2023 was implemented using likelihood algorithm, with the same number of samples for each class as in the visual case for the year 2013. In addition, the concordance matrix was calculated (Figure 5) to evaluate the quality of the adopted samples. It was found that all the assigned categories are located at a rate of more than 95% within different groups and that there is no overlap between categories by more than 4%.

ERROR MATRIX

| Classified Data | Reference Data: Buillt_Up | Vegetation | Water | Row Total |
|---|---|---|---|---|
| Buillt_Up | 96.04 | 4.30 | 0.51 | 552 |
| Vegetation | 3.96 | 95.70 | 0.51 | 424 |
| Water | 0.00 | 0.00 | 98.98 | 194 |
| Column Total | 555 | 419 | 196 | 1170 |

----- End of Error Matrix -----

Figure 5. Evaluation report on the accuracy of Landsat 8 visual training samples for the year 2023.

Therefore, the selected samples are considered acceptable. After ensuring the accuracy of the training samples, the imagery was classified using the maximum likelihood method. (Figure 6) shows the results of this classification. The classification accuracy was evaluated using the reference image that covers the study area. The confusion matrix or error matrix was generated using 100 check points measured on the classified imagery. Then, the file was opened, and these classified points were compared to the true reference points from the reference imagery. The overall accuracy for the classification reached 87.05%, while the kappa coefficient value was 0.89.

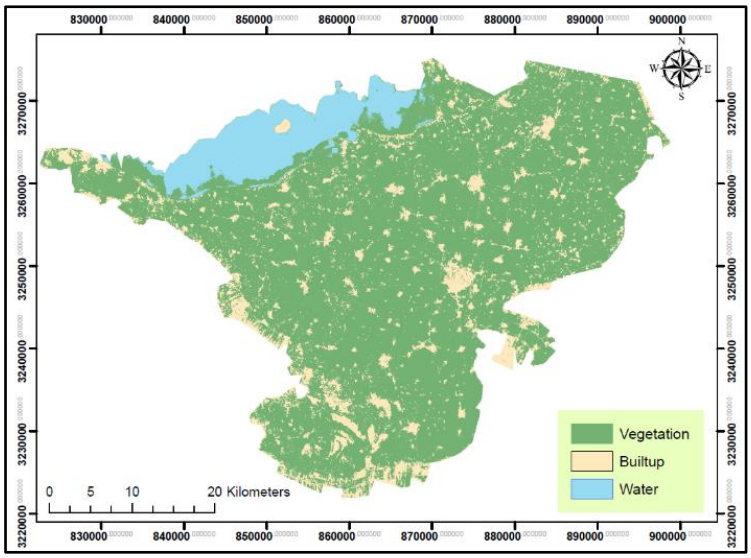


Figure 6. Results of Landsat 8 OLI maximum likelihood classification for the year 2023.

**5.3 Calculation of spectral indices for Landsat 8 OLI visible bands for the year 2013.**

Using the Raster Calculator tool available in ArcGIS 10.8 and equations 1, 2, and 3, the vegetation indices NDVI, NDBI, and NDWI were calculated, respectively, based on Landsat 8 OLI imagery for the year 2013. The results of these calculations are shown in the following figures (Figures 7, 8, and 9).

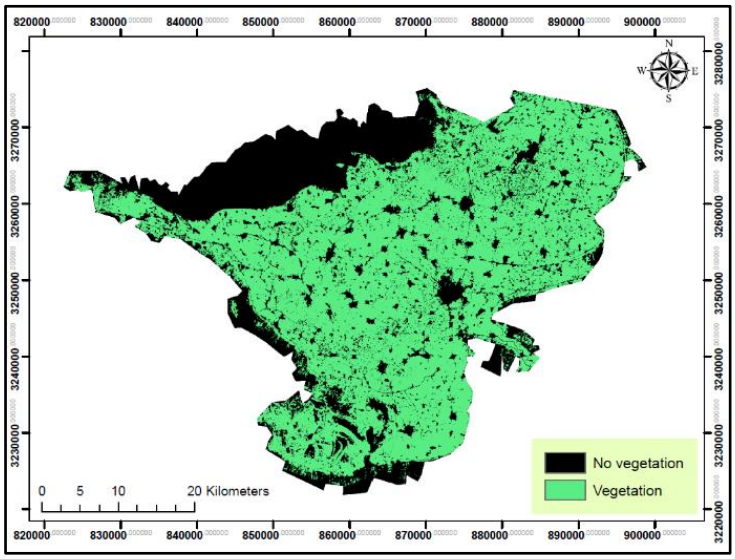


Figure 7. The NDVI index from the Landsat 8 OLI imagery for the year 2013.

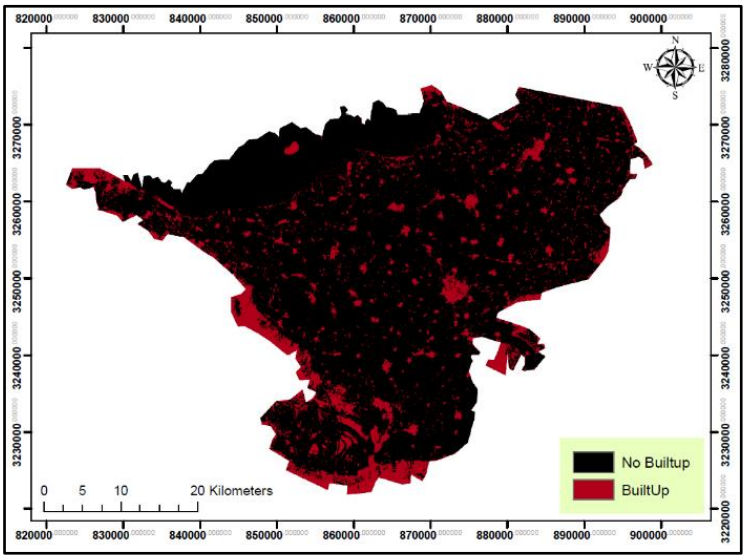


Figure 8. The NDBI index from the Landsat 8 OLI imagery for the year 2013.

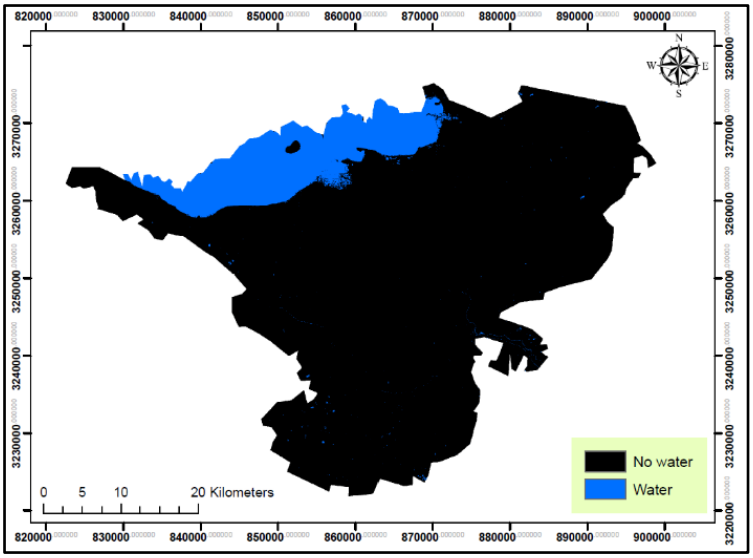


Figure 9. The NDWI index from the Landsat 8 OLI imagery for the year 2013.

### 5.4 Calculation of spectral indices for Landsat 8 visible bands for the year 2023.

As in the previous case, using the Raster Calculator tool available in ArcGIS 10.8 and equations 1, 2, and 3, the spectral indices NDVI, NDBI, and NDWI, were calculated respectively, using Landsat 8 imagery bands for the year 2023. The results of these calculations are shown in the following figures (Figure 10, 11 and 12):

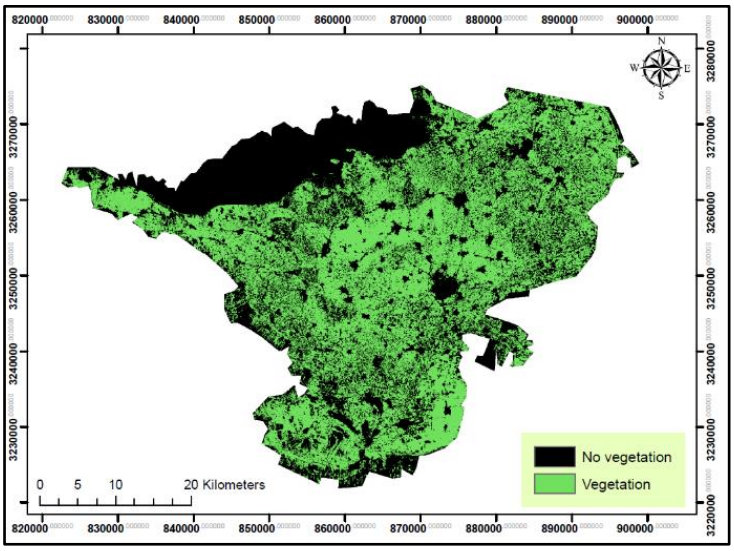


Figure 10. The NDVI index from the Landsat 8 OLI imagery for the year 2023.

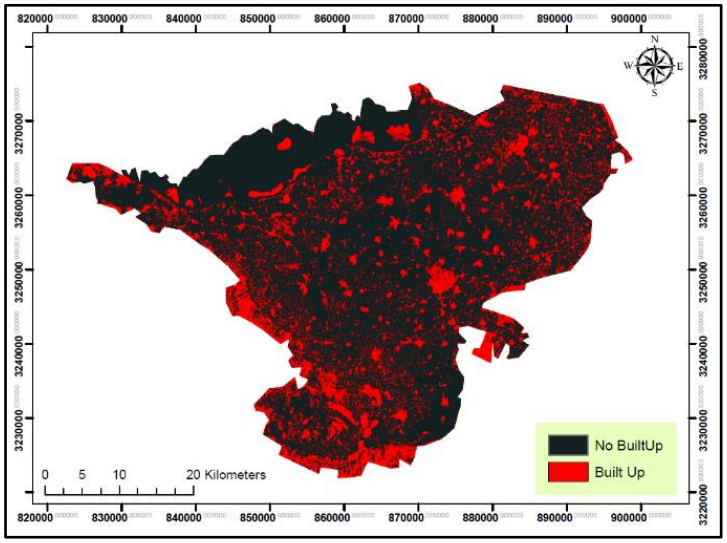


Figure 11. The NDBI index from the Landsat 8 OLI imagery for the year 2023.

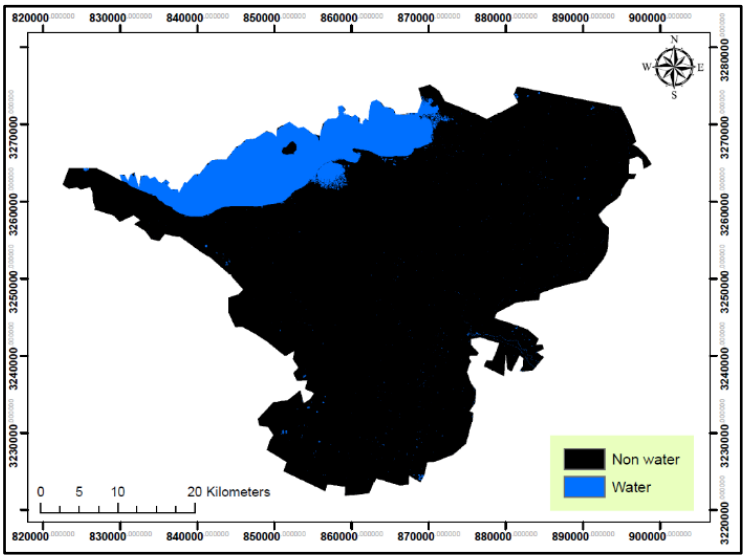


Figure 12. The NDWI index from Landsat 8 OLI imagery for the year 2023.

## 5.5 Results and Discussions.

*5.5.1 Results of land cover changes based on supervised classification.*

The results are shown in (Table 4) and (Figure 13), of the supervised classification of land cover using the maximum likelihood method for the years (2013) and (2023) for the city of Fayoum, Egypt, specifying the area in square kilometers and the percentage for each classification.

Table (4). The ground cover for 2013 and 2023 for the city Fayoum, resulting from the supervised classification, with areas and percentage ratios for the categories.

| Land cover type | 2013 | | 2023 | |
|---|---|---|---|---|
| | Area in $Km^2$. | (%) | Area in $Km^2$. | (%) |
| **Built-up (urban areas)** | 321.86 | 16.07 | 401.69 | 20.06 |
| **Vegetation** | 1437.48 | 71.79 | 1361.45 | 67.99 |
| **Water** | 242.95 | 12.13 | 239.15 | 11.94 |
| **Total** | 2002.29 | 100% | 2002.29 | 100% |

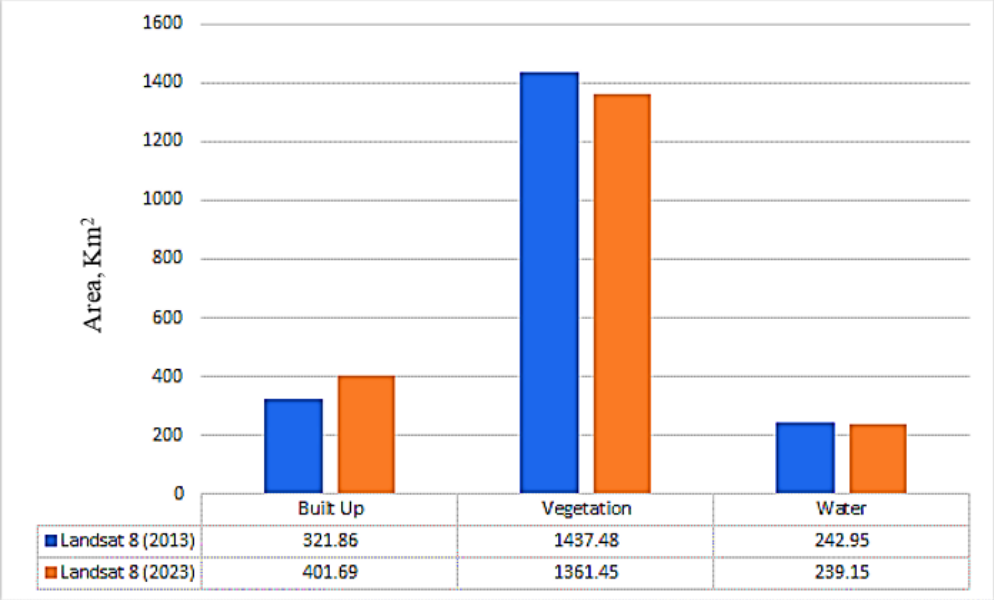


Figure 13. Comparison of the areas of land cover types resulting from the classification of Landsat 8 OLI imagery for the years 2013 and 2023 in square kilometres.

From (Table 4) and (Figure 13), it was found that; a decrease in green areas between the years 2013 and 2023 by 76.03 square kilometers, with a slight decrease in the area occupied by water amounting to 3.8 square kilometers. Meanwhile, there is an increase in the built-up areas by 79.83 square kilometers at the expense of green areas.

*5.5.2 Results of land cover changes based on spectral indices.*

The areas occupied by the studied and calculated categories based on the imagery representing the spectral indices NDVI, NDBI, and NDWI derived from Landsat 8 imagery for the years 2013 and 2023, respectively are shown in (Table 5) and (Figure 14).

Table (5). The land cover for the years 2013 and 2023 of the city of Fayoum resulting from the application of spectral indices along with the areas and percentage proportions of the categories.

| Land cover type | 2013 | | 2023 | |
|---|---|---|---|---|
| | Area in square kilometres. | (%) | Area in square kilometres. | (%) |
| **Built-up (urban areas)** | 311.242 | 15.54 | 405.71 | 20.26 |
| **Vegetation** | 1444.19 | 72.13 | 1353.07 | 67.58 |
| **Water** | 246.86 | 12.33 | 243.51 | 12.16 |
| **Total** | 2002.3 | 100% | 2002.3 | 100% |

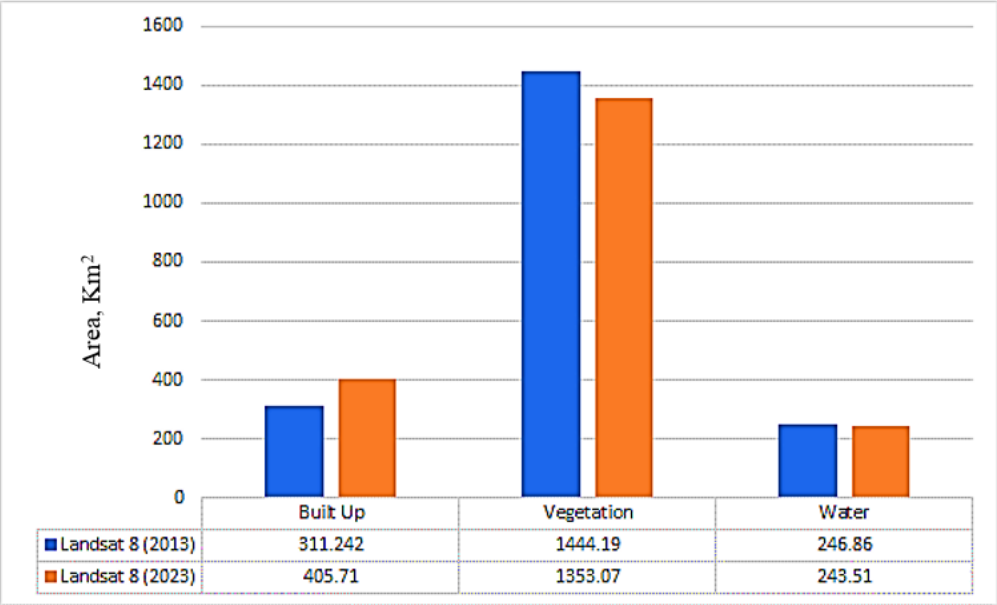


Figure 14. Comparison of the areas of categories resulting from the application of spectral indices on Landsat 8 imagery for the years 2013 and 2023 in square kilometres.

From (Table 5) and (Figure 14), it was found that; a decrease in green areas between the years 2013 and 2023 by an amount of 91.12 square kilometers, with a slight decrease in the areas occupied by water amounting to 3.35 square kilometers. Meanwhile, it was found that an increase in the built-up areas by 94.47 square kilometers at the expense of green lands.

### 5.6 Evaluation of the effectiveness of the indices in deriving land cover maps.

From the percentage changes in the areas of land cover categories during the study period (Tables 4 and 5), it was found that; the values are very close. In fact, the changes in the spatial extents occupied by land cover types during the study period resulting from visual classification can be used as reference values to assess the ability of spectral indices to detect changes in these areas within the same study period. Therefore, the values of changes in the areas of land cover types based on supervised classification were calculated and considered as a reference value for changes in the areas calculated by applying spectral indices. These values are specified in (Table 6) and (Figure 15).

Table (6). Areas of land cover types for the reference years (2013) and (2023), calculated using tested indicators along with the values of change in these areas between the years (2013) and (2023).

| Visual | Vegetation ($km^2$) | | Built-up (urban areas) ($km^2$) | | Water areas ($km^2$) | |
|---|---|---|---|---|---|---|
| | Reference area ($km^2$) | NDVI calculated area. ($km^2$) | Reference area ($km^2$) | NDBI calculated area. ($km^2$) | Reference area ($km^2$) | NDWI calculated area. ($km^2$) |
| **Landsat 2013** | 1437.48 | 1444.19 | 321.86 | 311.242 | 242.95 | 246.86 |
| **Landsat 2023** | 1361.45 | 1353.07 | 401.69 | 405.71 | 239.15 | 243.51 |
| **Change in area** | 76.03 | 91.12 | 79.83 | 94.468 | 3.8 | 3.35 |

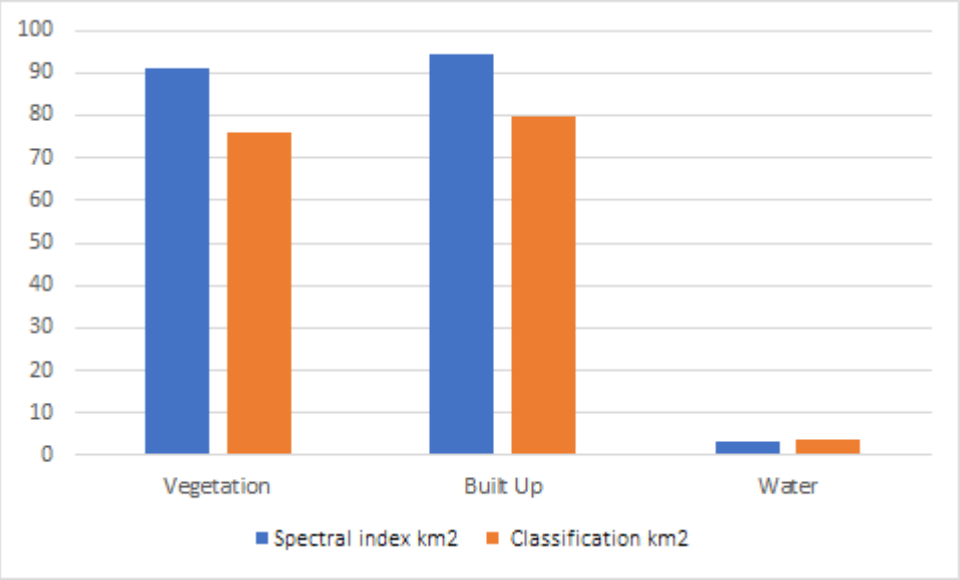


Figure 15. Comparison of changes in urban areas between the years (2013) and (2023) calculated using tested indicators with reference change values resulting from supervised classification.

From Table 6 and Figure 15, it was found that; an overall convergence in the changes of the areas of the adopted categories, with a significant convergence in the change in the water category area calculated by the NDWI index (the difference between the two areas is equal to 0.45 square kilometers), indicating the effectiveness of this index in identifying water surfaces. Additionally, a similarity was found in the effectiveness of both indicators NDVI and NDBI, where the difference in the case of the NDVI index reached a value of 14.46 square kilometers, while it reached 15.09 square kilometers in the case of the NDBI index.
Finally, the effectiveness of the tested spectral indices in this research has been evaluated by sampling land cover classes. The accuracy of the studied spectral indices was tested by measuring 100 check points in green areas, 100 check points in urban areas and bare lands, as well as 100 check points in areas covered by water bodies, using the supervised classifications for the years 2013 and 2023, respectively. Afterwards, the corresponding values for these points were extracted from the visuals of the spectral indices, namely NDVI, NDBI, and NDWI, which were calculated from these visuals. Finally, the percentage of check points were calculated corresponding to each category of the studied land cover classes (green areas, built-up areas, and water bodies) accurately. These percentages were considered as the value for the accuracy of the extraction of the studied spectral indices for the land cover classes.

Table (7). The accuracy of the tested spectral indices in extracting land cover classes in the study area.

| **Visual** | **NDVI** | **NDBI** | **NDWI** |
|---|---|---|---|
| Landsat 2013 | 80% | 68% | 94% |
| Landsat 2023 | 82% | 70% | 96% |

From (Table 7) it was found that; the high percentage of correctly determined check points specific to the indicator, while these percentages significantly decrease in the case of the spectral indices NDVI and NDBI. This can be interpreted in the case of the NDBI index due to the presence of several check points that corresponded to bare lands instead of buildings, which is confirmed by several previous reference studies [19] that have shown that distinguishing between built-up areas and bare lands using spectral indices is a very difficult process, despite the multiple suggestions and attempts to differentiate between them using multiple spectral indices.

## 6. Conclusion and recommendations

This research evaluated the effectiveness of using spectral indices in land cover classes and change detection in part of Fayoum Governorate between 2013 and 2023, using Landsat 8 OLI satellite images as an alternative to traditional supervised classification. The results demonstrated the ability of these indices to effectively detect land cover changes compared to the maximum likelihood supervised classification method. This encourages their use in various applications, such as natural resource management, urban planning, and more.

The values representing the normalized difference vegetation index (NDVI), the normalized difference building index (NDBI), and the Normalized Difference Water Index (NDWI) were calculated for the years 2013 and 2023. Then the supervised classification had been proceeded using the maximum likelihood algorithm, aiming to obtain reference visuals that are used to evaluate the effectiveness of the tested spectral indices and to obtain reference values for the urban areas, green areas, water bodies, and their changes in the study area during the studied time periods. The results indicate that the overall accuracy of the Landsat 8 visual classification for the year 2013 reached a value of 88.3% with a kappa coefficient of 0.90. Furthermore, the overall accuracy of the classification was 87.05% with a kappa coefficient of 0.89 when using Landsat 8 visual data for the year 2023.

As a result of the supervised classification, a decrease was observed in green areas between the years 2013 and 2023 by a magnitude of 76.03 square kilometers, with a slight decrease in the areas occupied by water by an amount of 3.8 square kilometers. Meanwhile, an increase was noticed in built-up areas by 79.83 square kilometers, at the expense of green lands. Moreover, the results of using spectral indices showed a decrease in green areas between 2013 and 2023 by 91.12 square kilometers, with a slight decrease in the areas occupied by water amounting to 3.35 square kilometers. Meanwhile, an increase was noticed in built-up areas by 94.47 square kilometers at the expense of green areas. The results showed a general convergence in the changes in the areas of the adopted categories during the study period, with a significant convergence in the change in the area of the water as computed by the NDWI index (the difference between the two areas is equal to 0.45 square kilometers). This indicates the effectiveness of this index. Meanwhile, a convergence was found in the effectiveness of both the NDVI and NDBI indices. Finally, the effectiveness of spectral indices was assessed in classifying land cover types using the concept of measured check points on the images of the indices and on the resulting images from the supervised classification for the years 2013 and 2023, respectively. The percentage of check points was calculated correctly corresponding to each class of the studied land cover types (green areas, built-up areas, and water bodies). The results showed a high percentage of correctly identified check points for the NDWI index (94% in 2013 and 96% in 2023), with a noticeable decrease in these percentages in the case of the spectral indices NDVI and NDBI.

Compared to previous studies, such as the study by Yasin et al. (2022) [16] and the study by Shoukat et al. (2022) [17], which also used a set of Landsat 8 OLI/TIRS images as in this research, it was found that; the results are consistent with the findings of these studies. They demonstrated the effectiveness of the spectral indices NDVI and NDBI in assessing urban growth temporally and spatially, and that the use of these indices improves the accuracy of land cover change analysis.

The study recommends using higher resolution imagery (such as Sentinel-2 imagery) to determine the impact of improved resolution on the effectiveness of the tested indices in deriving land cover maps and detecting changes. It also recommends developing new spectral indices or improving existing ones, particularly regarding the built-up area index, which practically does not differentiate between buildings and roads.

**References**

[1]. [MICHAEL. A, WULDER. NICHOLAS, C. COOPS. DAVID, P. ROY, JOANNE, C. WHITE. TXOMIN, H. - Land cover 2.0 - International Journal of Remote Sensing, Vol.39, 2018, pp 4254-4284.

[2]. YANG, D. FU, C. SMITH, A, C. YU, Q. - Open land-use map: A regional land-use mapping strategy for incorporating Open-StreetMap with earth observations - Geo-spatial Information Science, 2017, pp 269–281.

[3]. SHAHABI, H. SHIRZADI, A. GHADERI, K. OMIDVAR, E. AL-ANSARI, N. CLAGUE, JJ. GEERTSEMA, M. KHOSRAVI, K. AMINI, A. BAHRAMI, S. RAHMATI, O. - Flood detection and susceptibility mapping using sentinel-1 remote sensing data and a machine learning approach: hybrid intelligence of bagging ensemble based on K-nearest neighbor classifier - Remote Sens, Vol.12, 2020.

[4]. MINALE, A. - Retrospective Analysis of Land Cover and Use Dynamics in Gilgel Abbay Watershed by using GIS and Remote Sensing Techniques, Northwestern Ethiopia - International Journal of Geosciences, 2013, pp 1003-1008.

[5]. MORAN, E. SKOLE, D. TURNER, B. - The development of the international land –use and land cover change (LUCC) research program and its links to NASA'S land- cover and land use change (LCLUC) initiative – in Land change science: Observing, Monitoring and Understanding Trajectories of Change on the Earth's Surface, Netherlands: Kluwer Academic Publishers, 2004.

[6]. HALDER, A. GHOSH, A. GHOSH, S. - Supervised and unsupervised landuse map generation from remotely sensed images using ant-based systems - Appl Soft Comput, Vol.11, 2011, pp 5770–5781.

[7]. JOG, S. DIXIT, M. - Supervised classification of satellite images - in 2016 Conference on Advances in Signal Processing (CASP), IEEE, 2016, pp 93-98.

[8]. Akgün, A., Eronat, A. H., & Türk, N.- Comparing different satellite image classification methods: an application in Ayvalik District, Western Turkey. In The 4th international congress for photogrammetry and remote sensing, Istanbul, Turkey, Vol. 40, July 2004.

[9]. ROUSE, J.W., HAAS, R.H., SCHELL, J.A., DEERING, D.W. (1973) Monitoring Vegetation Systems in the Great Plains with ERTS (Earth Resources Technology Satellite). Proceedings of 3rd Earth Resources Technology Satellite Symposium, Greenbelt, 10-14 December, SP-351, 309-317.

[10]. ZHA, Y. GAO, J. NI, S. - Use of normalized difference built-up index in automatically mapping urban areas from TM imagery - International journal of remote sensing, Vol.24, 2003, pp 583-594.

[11]. FEYISA, GL. MEILBY, H. FENSHOLT, R. PROUD, SR. - Automated Water Extraction Index: A new technique for surface water mapping using Landsat imagery - Remote Sens. Environ, 2014, pp 23-35.

[12]. NGUYEN, C.T, et al. -A modified bare soil index to identify bare land features during agricultural fallow-period in southeast Asia using Landsat 8- Land, 2021, 10.3: 231.

[13]. SZABO, S. GACSI, Z. BALAZS, B. - Specific Features of Ndvi, Ndwi and Mndwi as Reflected in Land Cover Categories - Landscape & Environment, 2016, pp 194-202.

[14]. ABDEL-GAWAD, A., EL-BELBEISY, Analysis and detection of changes in land cover patterns and their comparison with land use map in Al-Muwaqqar district using satellite imagery and geographic information systems. Studies in humanities and social sciences, 46, 2019, 2: 246-266.

[15]. AL-KHAQANI AND IBTEHAL TAQI AL-DIN, Using the Normalized Difference Vegetation

Index (NDVI), Normalized Difference Water Index (NDWI), and Normalized Difference Built-up Index (NDBI) to detect changes in land cover for selected areas in Al-Najaf Governorate during the period between 2001 to 2006 using remote sensing data. Al-Kufa Journal of Physics, 6, 2, 2014, pp 12-18.

[16]. YASIN, M, Y. ABDULLAH, J. NOOR, N, M. YUSOFF, M, M. NOOR, N, M. - Landsat observation of urban growth and land use change using NDVI and NDBI analysis - in IOP Conference Series: Earth and Environmental Science, Vol.1067, 2022.

[17]. SHOUKAT, A, S. MADEEHA, K. ALEENA, N. SHAHARYAR, H, A. - Exploring NDVI and NDBI Relationship Using Landsat 8 Oli/Tirs in Khangarh Taluka, Ghotki - Malaysian Journal of Geosciences, Vol.6, 2022, pp 08-11.

[18]. SINHA, P. VERMA, N, K. AYELE, E. - Urban built-up area extraction and change detection of Adama municipal area using time-series Landsat images - International Journal of Advanced Remote Sensing and GIS, Vol.5, 2016, pp 1886-1895.

[19]. Li, H., WANG, C., ZHONG, C., SU, A., XIONG, C., WANG, J., LIU, J. Mapping Urban Bare Land Automatically from Landsat Imagery with a Simple Index. Remote Sens. 2017, 9, 249

[20]. MINISTRY OF HOUSING, Utilities, and Urban Communities, General Organization for Urban Planning. 2017- Future Vision and Supporting Projects for the Development of Fayoum Governorate. 6-10.

[21]. SHAHI, A, P. RAI, P, K. MISHRA, V, N. - Remote sensing data extraction and inversion techniques: A review - Atmospheric Remote Sensing, 2023, pp 85-104.

[22]. SONAWANE, K. BHAGAT, V. - Improved change detection of forests using Landsat TM and ETM+ data - Remote Sensing of Land, Vol.1, 2017, pp 18-40.

[23]. CHEN, F. YANG, S. YIN, KAI. CHAN, P. - Challenges to quantitative applications of Landsat observations for the urban thermal environment - J. Environ. Eng. 3 (59), 2017, pp 80-88.

[24]. SHAH, S, A. SIYAL, A, A. - GIS-based approach estimation of area under wheat and other major rabi crops in district Ghotki and corresponding irrigation water requirements - Acta Scientific Agriculture, Vol.3, 2019, pp 59-70.

[25]. SHAH, S, A. KIRAN, M. KHURSHID, T. - Seepage losses measurement of Desert minor and development of gauge-discharge rating curve: A case study in district Ghotki, Sindh - World Academics Journal of Engineering Sciences, vol.8, 2021, pp 13-22.

[26]. MALIK, M.S. SHUKLA, J.P. MISHRA, S. - Relationship of LST-NDBI and NDVI using Landsat 8 data in Kandaihimmat Watershed, Hoshangabad, India - Indian J. Geo-Marine Sci, Vol.48, 2019, pp 25-31.

[27]. XU, H. - A new index for delineating built-up land features in satellite imagery - International Journal of Remote Sensing, Vol.29, 2008, pp 4269–4276.

[28]. HANQIU, X. - Modification of normalized difference water index (NDWI) to enhance open water features in remotely sensed imagery - International Journal of Remote Sensing, 27, 14, 2006, pp 26-35.

[29]. DOXANI G, VERMOTE E, ROGER J-C, GASCON F, ADRIAENSEN S, FRANTZ D, HAGOLLE O, HOLLSTEIN A, KIRCHES G, LI F, et al. Atmospheric Correction Inter-Comparison Exercise. Remote Sensing. 2018; 10(2):352.

[30]. SANTAMARIA-ARTIGAS, A., VERMOTE, E. F., FRANCH, B., ROGER, J. C., & SKAKUN, S., Evaluation of the AVHRR surface reflectance long term data record between 1984 and 2011. International Journal of Applied Earth Observation and Geoinformation, 98, 102317, 2021.

[31]. AL-KHALIL, A., Criteria for verifying the geometric accuracy of geometric correction for

satellite images. Journal of Tishreen University for Research and Scientific Studies- Humanities Series Volume (38) Issue (2), 2016, 44, 29.

# تقييم دقة استشعار تغيرات الغطاء الأرضي باستخدام المؤشرات الطيفية والتصنيف الطيفي– حالة دراسة محافظة الفيوم في مصر

**ملخص**

تعدّ المؤشرات الطيفية المطورة لاقتطاع الظاهرات من المرئيات الفضائية من الأساليب البسيطة والسريعة والتي تقلل وقت المعالجة وذلك مقارنةً بالأساليب التقليدية لتصنيف المرئيات الفضائية. تم في هذا البحث تقييم فعالية مؤشرات نمو المنطقة الحضرية المعياري (NDBI) ومؤشر الاختلافات الخضرية المعياري NDVI ومؤشر المياه المعياري NDWI في اشتقاق خرائط الغطاء الأرضي واستشعار تغيراته في الفترة الزمنية الممتدة بين العامين 2013 و2023 في محافظة الفيوم في جمهورية مصر العربية باستخدام مرئيات Landsat 8–OLI. بيّنت نتائج التصنيف المراقب للمرئيات تراجع مساحة المناطق الخضراء بين عامي 2013 و2023 بمقدار 76.03 كيلومتر مربع مع تراجع بسيط في المساحات التي تشغلها المياه بلغت قيمته 3.8 كيلومتر مربع، في حين لاحظنا زيادةً في مساحة المناطق المبنية قيمته 79.83 كيلومتر مربع وذلك على حساب الأراضي الخضراء. من ناحية أخرى، لاحظنا عند استخدام المؤشرات الطيفية تراجع مساحة المناطق الخضراء بين عامي 2013 و2023 بمقدار 91.12 كيلومتر مربع مع تراجع بسيط في المساحات التي تشغلها المياه بلغت قيمته 3.35 كيلومتر مربع، في حين لاحظنا زيادةً في مساحة المناطق المبنية قيمته 94.47 كيلومتر مربع وذلك على حساب الأراضي الخضراء. بيّنت النتائج وجود تقارب عام في تغيرات مساحات الأصناف المعتمدة خلال فترة الدراسة مع الإشارة إلى التقارب الكبير في تغير مساحة صنف المياه المحسوب بالتصنيف وبتطبيق المؤشر NDWI في حين وجدنا تقارباً في فعالية كل من المؤشرين NDVI وNDBI. تم أخيراً تقييم فعالية المؤشرات الطيفية في تخريط الغطاء الأرضي باستخدام نقاط اختبار حيث بينت النتائج وجود نسبة مئوية عالية من نقاط الاختبار المحددة بشكل صحيح والخاصة بالمؤشر NDWI مع تدني هذه النسبة بشكل ملحوظ في حالة المؤشرين الطيفيين NDVI وNDBI.

**كلمات مفتاحية:** مرئيات فضائية، غطاء أرضي، مؤشرات طيفية، استشعار تغيرات، تصنيف مراقب.